Supplement of

Comparison of equatorial wave activity in the tropical tropopause layer and stratosphere represented in reanalyses

Young-Ha Kim et al.
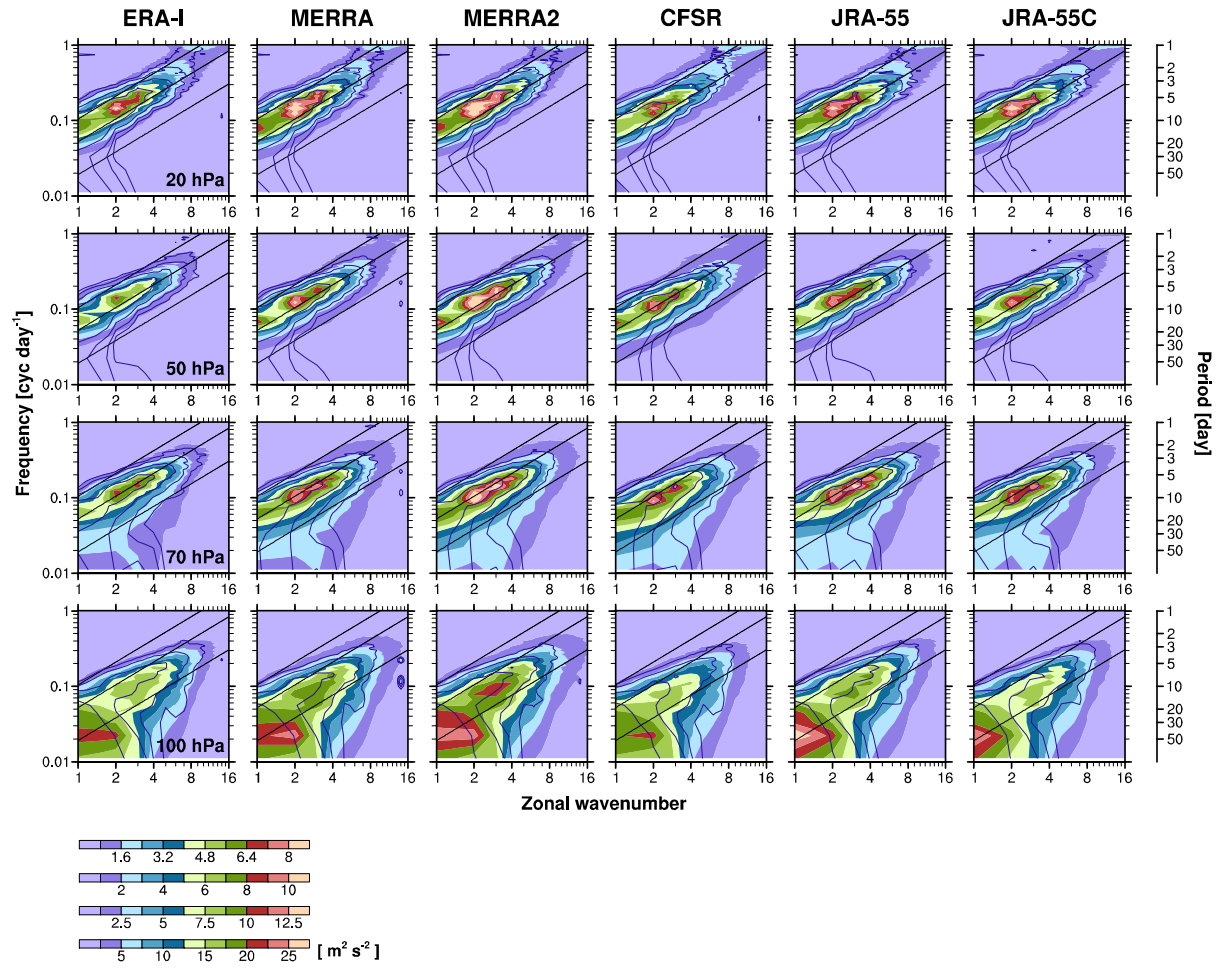
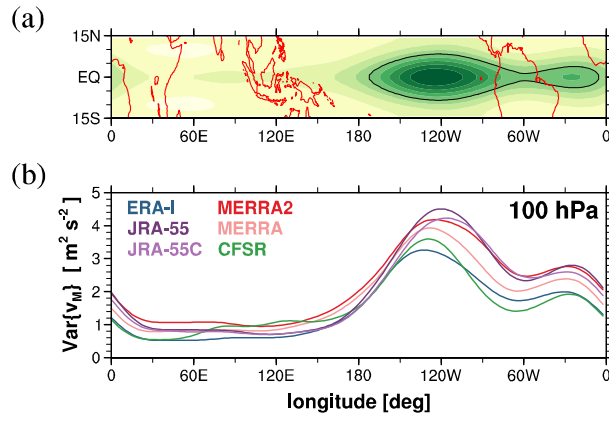**Figure S1.** The same as in Fig. 1 except for the zonal wind.

Figure S2. The same as in Fig. 3 except for the 100-hPa symmetric meridional wind filtered for $-10 \leq k < 0$ and $0.033 \leq \omega < 0.1 \, \mathrm{cyc \, day^{-1}}$.
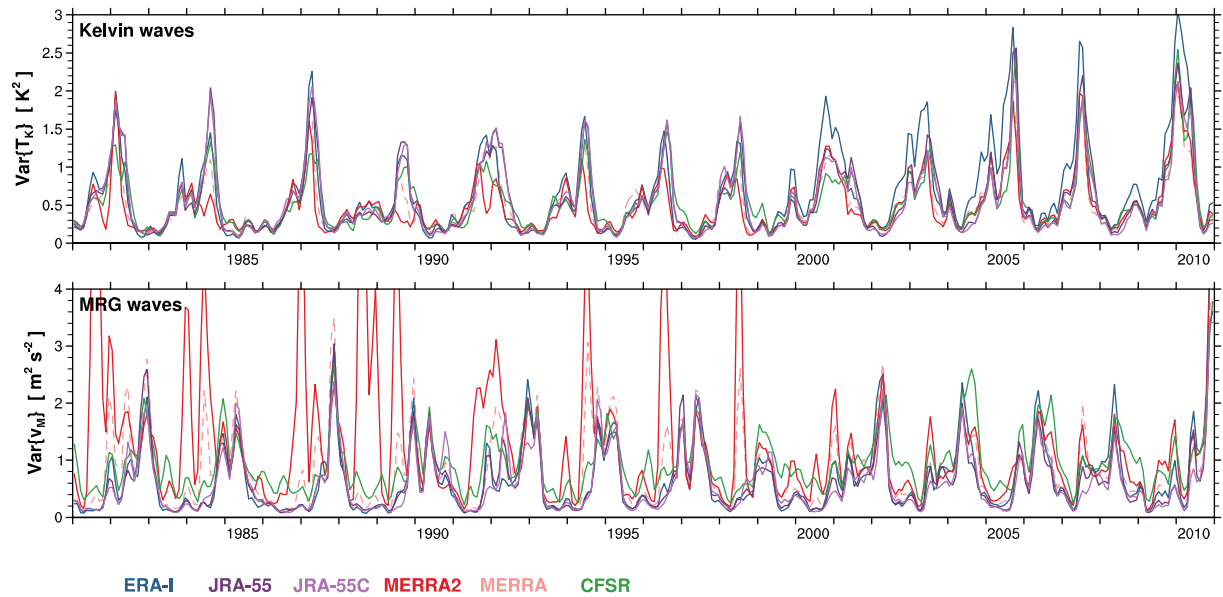
Figure S3. Monthly time series of variances of (upper) temperature for the Kelvin waves (T_{Kelvin}) and (lower) meridional wind for the MRG waves (v_{MRG}) at $10\,\mathrm{hPa}$ averaged over $15°\mathrm{N}$–$15°\mathrm{S}$. The MERRA results are from the standard-level datasets (dashed), and the others from the model-level datasets (solid). See the text in Section 3.1 for the definitions of T_{Kelvin} and v_{MRG}.
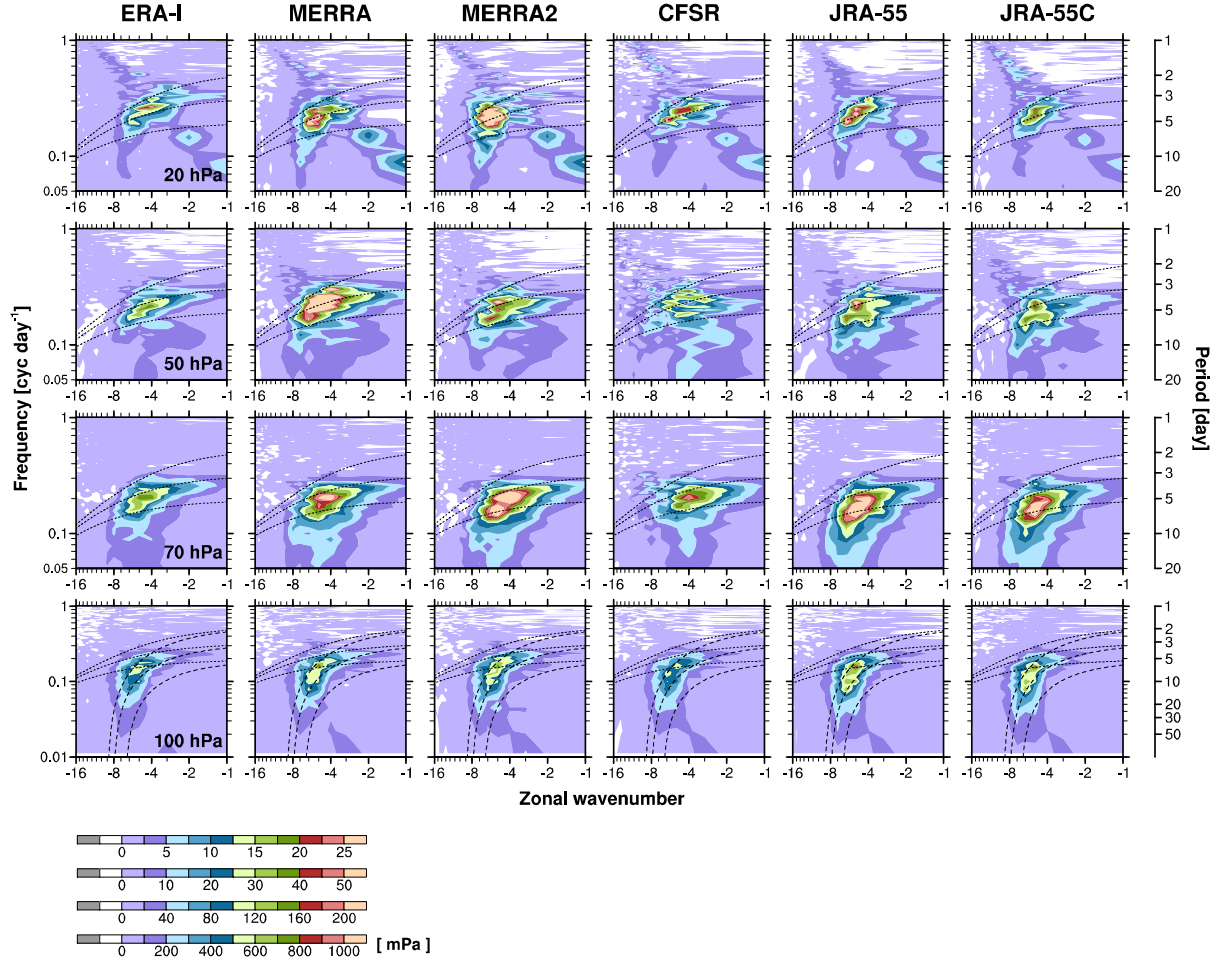
Figure S4. The same as in Fig. 10 except for $\langle F_\phi \rangle$ of antisymmetric modes over 5°N–5°S, where $\langle F_\phi \rangle$ is the latitudinal average of the equatorward EP flux, $\mathrm{sgn}(-\phi)F_\phi$, and ϕ the latitude.
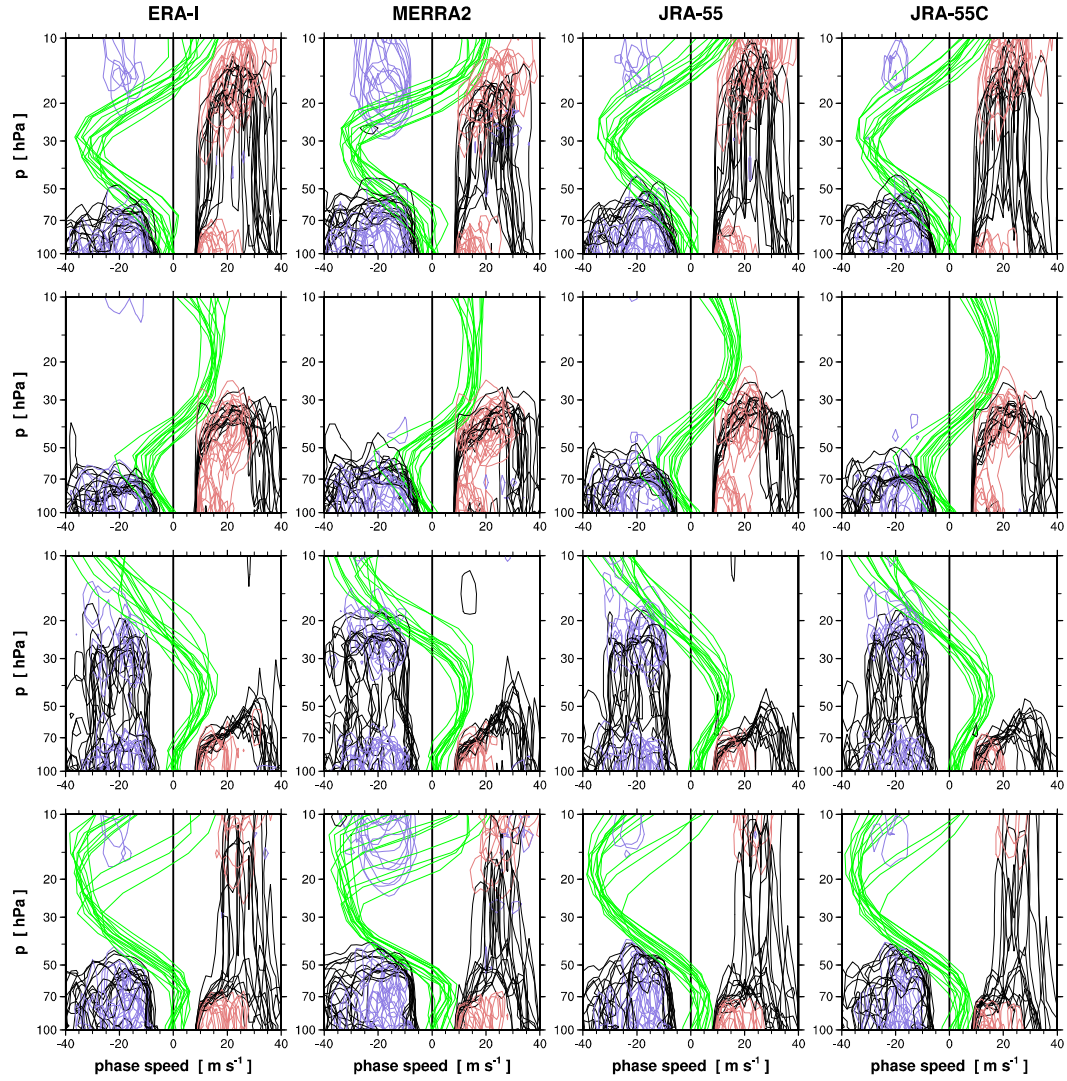
Figure S5. Spaghetti plots for 13 individual QBO cycles within the period of 1981–2010: contours for the Kelvin wave EP flux divergence of $0.3\,\mathrm{m\,s^{-1}\,month^{-1}/(m\,s^{-1})}$ (red), for the MRG wave EP flux divergence of $-0.06\,\mathrm{m\,s^{-1}\,month^{-1}/(m\,s^{-1})}$ (blue), and for the Kelvin and MRG wave F_z (black) of -0.008 and $0.0003\,\mathrm{mPa/(m\,s^{-1})}$, respectively, as a function of phase speed, during the four QBO phases shown in Fig. 11 (from top to bottom). The zonal-mean zonal-wind profiles are also plotted (green).